Synthesis and Characterization of Interpenetrating Polymer Networks from Polyurethane and Poly(ethylene glycol) Diacrylate

Hua Jin,[1] Sung Soo Yoon,[2] Sung Chul Kim[1]

[1]*Department of Chemical and Biomolecular Engineering, Korea Advanced Institute of Science and Technology, 373-1, Guseong-dong, Yuseong-gu, Daejeon 305-701, Korea*
[2]*Chemical and Polymers Research and Development, LG Chemicals, Limited, P.O. Box 61, Yu Sung, Science Town, Daejeon 305-380, Korea*

Received 18 April 2007; accepted 13 January 2008
DOI 10.1002/app.28094
Published online 8 April 2008 in Wiley InterScience (www.interscience.wiley.com).

ABSTRACT: Interpenetrating polymer networks (IPNs) combining polyurethane (PU) and poly(ethylene glycol) diacrylate (PEGDA) networks were prepared with simultaneous polymerization. PU was synthesized from biocompatible and biodegradable poly(ε-caprolactone) diol, and the hydroxyl group of poly(ethylene glycol) was substituted with a crosslinkable acrylate group. The effects of the PU/PEGDA compositions and the crosslink density of PU and PEGDA on the thermal properties, swelling ratio, surface energy, mechanical properties, and morphologies were investigated. The mechanical properties of PEGDA networks were improved by the presence of PU networks, particularly in the 75% PU/25% PEGDA IPNs. All PU/PEGDA IPNs showed a microphase-separated structure with cocontinuous morphology, as observed by atomic force microscopy, which was in agreement with the results of swelling ratio and dynamic mechanical thermal analysis measurements. © 2008 Wiley Periodicals, Inc. J Appl Polym Sci 109: 805–812, 2008

Key words: crosslinking; morphology; networks; polyurethanes

INTRODUCTION

Multiphase polymeric materials exhibit properties that are often superior to those of their component homopolymers because of their morphological structure.[1–5] Interpenetrating polymer networks (IPNs) are defined as a combination of two polymers in network form, at least one of which is crosslinked in the presence of the other.[6] IPNs are classified as sequential IPNs, simultaneous IPNs (SINs), and latex IPNs. Among these IPNs, SINs are generally the best for a high degree of intermixing because of the compatibility of the monomeric mixture, which is much higher than that of the polymeric mixture.[7] IPNs have gained widespread acceptance in applications as damping materials,[8] biomedical materials,[9] gas-transport membranes,[10] ion-exchange resins, and automotive bumpers.[11]

Polyurethanes (PUs), a class of very useful and versatile materials, have been widely used as individual polymers possessing a network structure because of their good flexibility and elasticity or as components of IPNs. Cooper and coworkers[12–15] reported that PUs having microdomain structures exhibited excellent blood compatibility in comparison with other polymeric materials. Therefore, they are extensively used in blood-contact and organ reconstruction applications. However, PUs are also known to be prone to surface cracking, stress-induced degradation, biodegradation, and calcification.[16] Therefore, since 1994, much research on hydrophilic PU/hydrophobic polystyrene (PS) IPNs has been reported by Kim and coworkers.[17–22] They found that amphiphilic PU/PS IPN materials exhibit good blood compatibility as well as excellent mechanical properties because the amphiphilic character is very useful in the suppression of the adhesion of blood coagulation factors by prohibiting the glycoproteins from excessively accumulating on a local position of the surface.

However, like most synthetic biomaterials, hydrophilic PU/hydrophobic PS IPNs might have problems in long-term clinical use. Therefore, new biocompatible IPNs based on PU and poly(ethylene glycol) diacrylate (PEGDA) were proposed by our research group.[23] Because poly(ethylene glycol) (PEG) has received much attention as a biomaterial on account of its low interfacial energy with water (hydrophilicity), lack of binding sites for reactive proteins, high chain mobility, and steric stabilization effects, it has been reported that PEG-treated biomaterials show less protein adsorption and good cell adhesion.[24] As a result, in PU/PEGDA IPNs, protein

Correspondence to: S. C. Kim (kimsc@kaist.ac.kr).

adsorption and platelet adhesion decrease as the molecular weight of PEGDA decreases, and they show good biocompatibility. On the basis of the previous research, in this study, we synthesized biocompatible hydrophobic PU/hydrophilic PEGDA IPNs using the SIN method[25–27] to investigate the thermal properties, mechanical properties, and morphologies of IPNs with respect to the composition and crosslink density of PU. Furthermore, the phase domain size and phase continuity of the polymer components were examined.

EXPERIMENTAL

Materials

Poly(ε-caprolactone) diol (weight-average molecular weight = 530 g/mol; Aldrich, St. Louis, MO) and PEG (weight-average molecular weight = 1000 or 2000 g/mol; Aldrich) were degassed at 60°C *in vacuo* overnight before use. 1,4-Butanediol (1,4-BD; Aldrich) as a chain extender and trimethylopropane (TMP; Aldrich) as a crosslinking agent were also degassed for 12 h *in vacuo* to remove moisture before use. Hexamethylene diisocyanate (HDI; TCI), acryloyl chloride (Aldrich), triethylamine (TEA; Aldrich), and benzene (Aldrich; anhydrous-grade) were used without further purification. Benzoin (Aldrich) was used as the photoinitiator, and dibutyltin dilaurate (T-12, Aldrich) was stored in a refrigerator before use as a PU catalyst.

Synthesis

Synthesis of PEGDA

Crosslinkable PEGDA was prepared by the substitution of the hydroxyl end group of PEG with an acrylate group.[23] First, 60 g of degassed PEG was dissolved in 600 mL of benzene. TEA, in a 3-fold molar excess based on the hydroxyl groups of PEG, was also dissolved in the PEG solution. Acrylolyl chloride, in a 3-fold molar excess based on the hydroxyl groups of PEG, was dissolved in benzene and added dropwise to the PEG solution at room temperature. The solution was stirred overnight at 35°C under nitrogen. The solution was filtered with Celite 545 to remove triethylamine hydrochloride salt, and the filtrate was precipitated in *n*-hexane twice. The precipitated PEGDA was dried at room temperature for more than 24 h *in vacuo* to remove excess solvent. Two kinds of PEGDAs were synthesized: PEGDA1K with PEG with a molecular weight of 1000 and PEGDA2K with PEG with a molecular weight of 2000.

Synthesis of the PU prepolymer

The NCO-terminated PU prepolymer was prepared by the reaction of 1 equiv of poly(ε-caprolactone) diol with 2 equiv of HDI at 65°C for 1.5 h under a nitrogen atmosphere.[23] Dibutyltin dilaurate (0.05 wt %) as a catalyst was added to poly(ε-caprolactone) diol before the reaction. HDI was charged into a four-necked flask and was heated to 65°C, and then the degassed poly(ε-caprolactone) diol was slowly dropped into HDI through a dropping funnel with vigorous stirring of the mixture. The reaction was stopped when the theoretical NCO percentage was reached (measured by the di-*n*-butylamine titration method).[26] The product was kept below 0°C after N_2 purging.

Synthesis of PU/PEGDA IPNs

The PU prepolymer, 1,4-BD, and TMP were poured into a 250-mL beaker, and then PEGDA was added at the desired weight ratios (100/0, 75/25, 50/50, 25/75, and 0/100) together with 1 wt % benzoin on the basis of the weight of PEGDA. The blends were mixed with a high-torque stirrer for 3 min and degassed for 30 s to remove the air bubbles entrapped during mixing. The homogeneous mixture was cast into a glass plate mold with a silicon spacer (1 mm thick), and the PU network and PEGDA network were synthesized simultaneously in a UV chamber at 80°C for 5 h.[23] The equivalent ratio of 1,4-BD and TMP to isocyanate was adjusted to give a theoretical molecular weight between crosslinks (M_c) of 1000 or 2000.

Characterization

Differential scanning calorimetry (DSC)

The thermal behavior of the PU network and PEGDA network was investigated with a TA Instruments (San Jose, CA) Q100 differential scanning calorimeter operating at a heating and cooling rate of 10°C/min under a nitrogen atmosphere from −70 to 150°C. Transitions were recorded from the heating scans with a linear extrapolation method (melting temperature) and the midpoint inflection method [glass-transition temperature (T_g)].

Dynamic mechanical thermal analysis (DMTA)

DMTA was carried out on a Rheometric Scientific (Piscataway, NJ) DMTA IV dynamic mechanical thermal analyzer. The tests were conducted from −100 to 70°C at a frequency of 1 Hz and a heating rate of 5°C/min. The sample size was 3 cm × 1 cm × 1.2 cm. The maximum loss factor (tan δ) was taken as T_g.

Tensile testing

The stress–strain properties of IPNs were measured with an Instron (Norwood, MA) 5583 machine. The

stress–strain measurement was conducted as described in ASTM D 638 with a crosshead speed of 5 mm/min. At least four specimens were used for the test.

Swelling behavior in water

IPNs were dried at room temperature for 24 h *in vacuo* and then immersed in distilled water until they were equilibrated with water. The weight of the sample was measured every 15 min, and the swelling ratio was calculated with the following equation:

$$\text{Swelling ratio} = \frac{W_s - W_d}{W_d}$$

where W_s is the weight of the swollen sample and W_d is the weight of the dry sample.

Interfacial energy

The interfacial energy between the surface of the IPN and water was measured with the underwater captive bubble technique.[21] The samples were equilibrated with distilled water for more than 24 h, and the static bubble contact angles of the surface, water, and air and surface, water, and hexane were then measured with a contact-angle goniometer (model G-I type, Erma, Tokyo, Japan) equipped with an oil droplet apparatus in the water. The interfacial energy between the surface and water was calculated with the harmonic mean equation:[28–30]

$$\gamma_{12} = \gamma_1 + \gamma_2 - 4\left(\frac{\gamma_1^d \gamma_2^d}{\gamma_1^d + \gamma_2^d}\right) - 4\left(\frac{\gamma_1^p \gamma_2^p}{\gamma_1^p + \gamma_2^p}\right)$$

where γ is the interfacial tension, γ^d is the dispersion component, and γ^p is the polar component.

Atomic force microscopy (AFM)

The nanostructured morphology of the cross section of the IPN was acquired with a Digital Instruments Multimode Nanoscope IIIa from Veeco (Santa Barbara, CA). The instrument was equipped with an E scanner and operated in air. For tapping-mode AFM, a commercial silicon cantilever (tapping mode etched silicone probe (TESP) tip), 125 μm long, from Digital Instruments was used. The spring constant was set from 20 to 100 N/m, and the frequency was set at 1 Hz.

RESULTS AND DISCUSSION

Thermal characterization

Dynamic mechanical analysis data can be used to study the degree of mixing in IPN materials. In a tan δ/temperature plot, a narrow peak of tan δ indicates a high degree of mixing, whereas two clearly separated peaks with a low value of tan δ between the two peaks indicate a large degree of phase separation. The intermediate situation for an intermediate degree of mixing in IPNs is represented by a single broad transition. Two peaks of tan δ of the same height may be indicative of two continuous phases.[31]

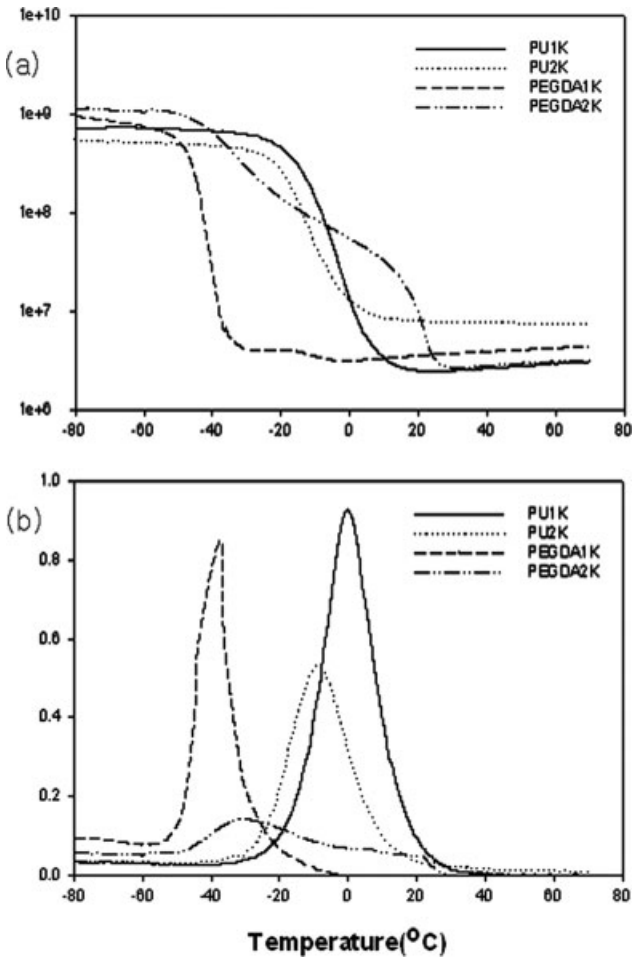

Figure 1 (a) E' and (b) tan δ versus the temperature for the single networks.

The storage modulus (E') and tan δ versus temperature are reported in Figure 1(a,b) for the PEGDA and PU homonetworks. Two significant differences are observed in the PEGDA1K and PEGDA2K homonetworks and PU1K and PU2K homonetworks (PU1K means the PU homonetwork with M_c = 1000). First, the modulus in the rubbery plateau is much higher for the PEGDA1K homonetwork than for the PEGDA2K homonetwork because of the higher crosslink density of the PEGDA1K network. However, despite the lower crosslink density of PU2K, the modulus in the rubbery plateau for PU2K is much higher than that for the PU1K homonetwork [Fig. 1(a)]. The increase in the modulus can be explained by the existence of crystallites inside the PU2K network, as observed in the DSC results (Fig.

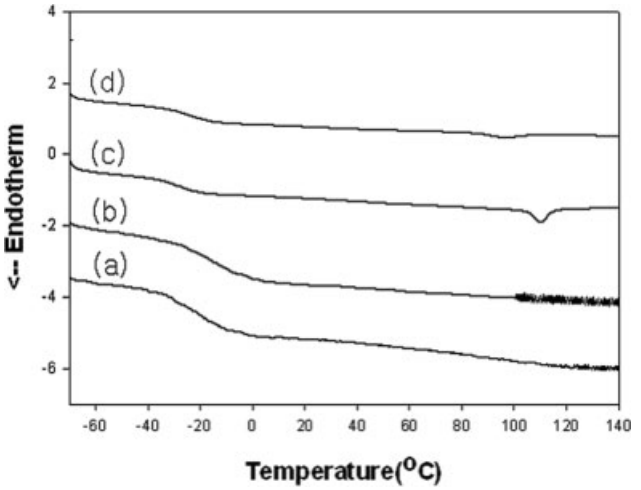

Figure 2 DSC thermograms of (a) the PU1K network in the first heating run, (b) the PU1K network in the second heating run, (c) the PU2K network in the first heating run, and (d) the PU2K network in the second heating run.

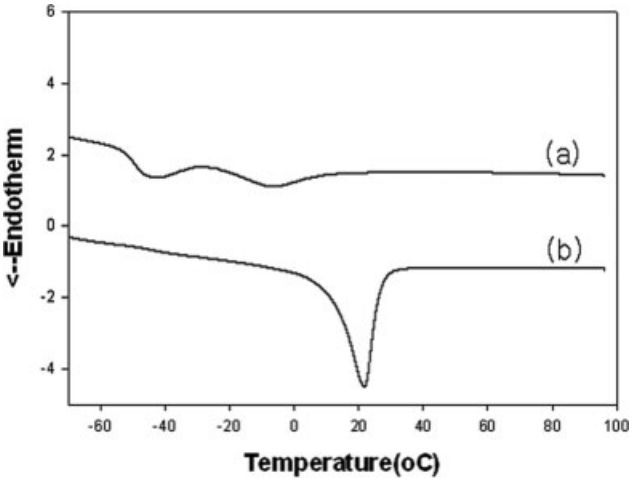

Figure 3 DSC thermograms of (a) the PEGDA1K network in the second heating run and (b) the PEGDA2K network in the second heating run.

2). As indicated by the DSC thermogram, PU1K is amorphous in nature and shows only the glass transition in the first and second heating runs [Fig. 2(a,b)]. PU2K, in the first heating run, shows the glass transition around −27°C and the melting endotherm at 110.8°C [Fig. 2(c)]; however, the second heating after cooling from 150°C results in the glass transition at a temperature (−23°C) higher than that of the first heating scan, and a small melting transition at 96°C can be observed [Fig. 2(d)]. A slow crystallization rate is suggested as PU2K is cooled from the melt. Second, the α relaxation of the PEGDA2K homonetwork is very broad, as evidenced by the tan δ peak, which ranges over more than 50°C with a maximum value of approximately −30°C [Fig. 1(b)], in comparison with that of the PEGDA1K homonetwork. This is probably due to the nonhomogeneity in the crosslink density in the PEGDA2K homonetwork. E' of the PEGDA2K network suddenly drops around 20°C [Fig. 1(b)], and this indicates the melting of the PEG crystalline segment because the molecular weight of PEG is higher for the PEGDA2K network. A strong melting peak at 22°C can also be observed in PEGDA2K, as shown in the DSC thermogram [Fig. 3(b)].[32]

The viscoelastic behavior of IPNs has been also characterized with DMTA. Figures 4 and 5 show the corresponding variations of tan δ versus the temperature. All IPNs with PEGDA1K [Figs. 4(a) and 5(a)] show dual-phase morphology evidenced by two partially demixed mechanical relaxations. However, the IPNs with PEGDA2K [Fig. 4(b) and 5(b)] show a single broad tan δ peak that is shifted to a temperature between the T_g values of the PU# and PEGDA2K homonetworks. The broad but single peak of the IPN indicates a high degree of interpenetration between both partner networks, as shown in the AFM studies later, indicating better miscibility between PU and PEGDA networks. In addition, de-

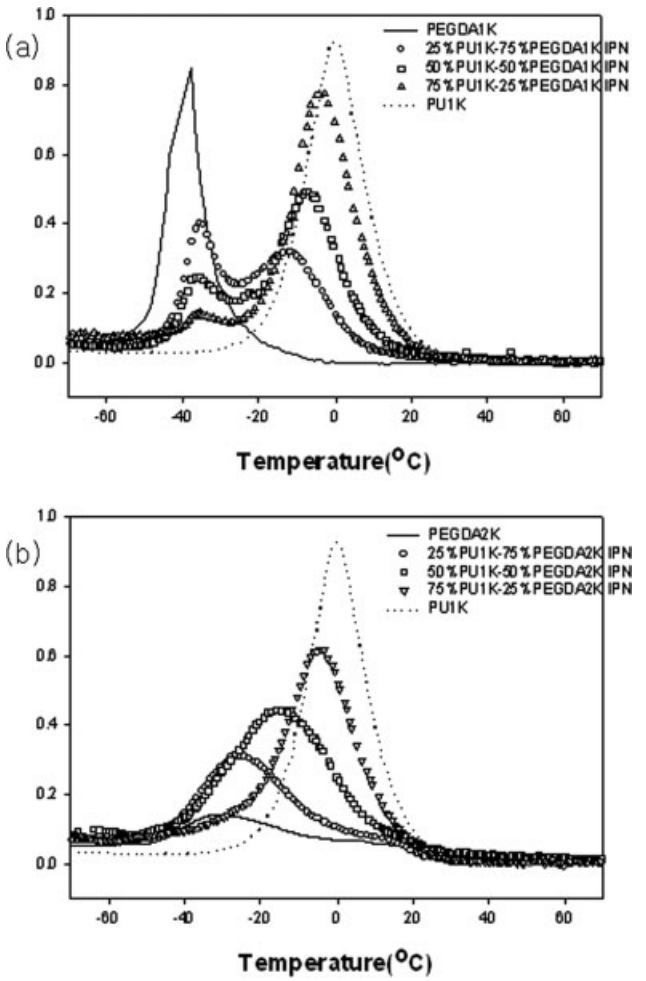

Figure 4 Tan δ versus the temperature for (a) the PU1K/PEGDA1K IPNs and (b) the PU1K/PEGDA2K IPNs.

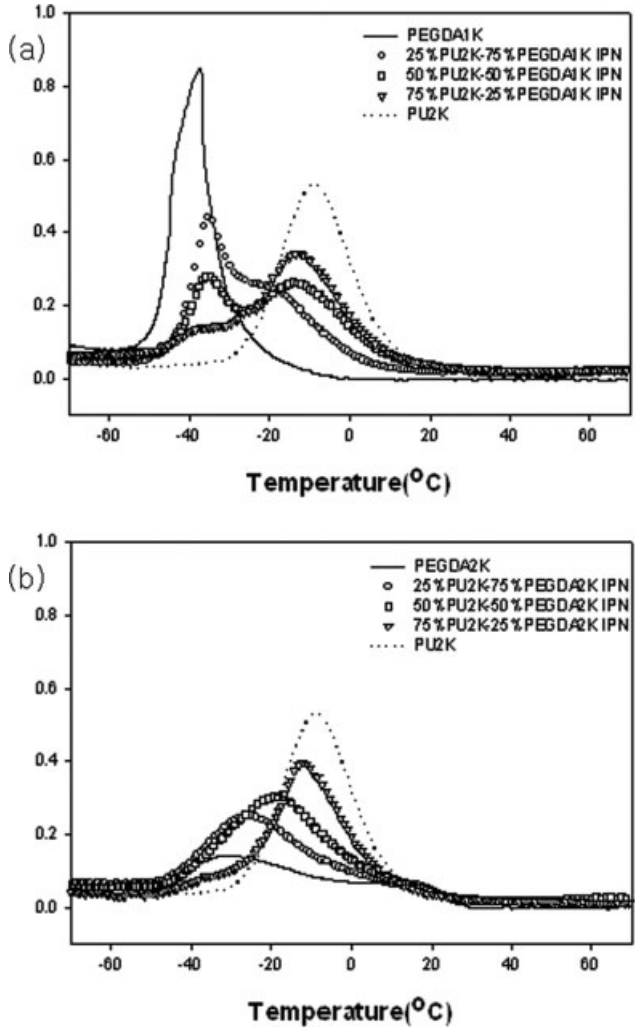

Figure 5 Tan δ versus the temperature for (a) the PU2K/PEGDA1K IPNs and (b) the PU2K/PEGDA2K IPNs.

spite the higher crosslink density of the PEGDA1K homonetwork, it shows a lower value of T_g (−37.6°C) than the PEGDA2K homonetwork (−30.6°C). The reason that PEGDA2K shows a higher T_g value than the PEGDA1K homonetwork is the pronounced crystallite formation in the network chains, as evidenced by the strong melting peak at 22°C in Figure 3(b).

Mechanical properties

The mechanical properties of the composition series were investigated with tensile testing measurements. The stress–strain data for PU/PEGDA IPNs are summarized in Tables I and II. In the case of PU2K/PEGDA2K IPNs (Table I), when the PU content increases from 0 to 50 wt %, the tensile strength and elongation at break gradually increase from 0.9 MPa and 16% to 2.0 MPa and 29%, respectively. However, the tensile strength and elongation at break increase dramatically to 6.5 and 158% when the PU content is 75% for the PU2K/PEGDA2K IPN. This increase in the tensile strength can be explained by the phase continuity of the IPNs, as the continuous phase is known[6] to have a large influence on the mechanical properties of IPNs. Increasing the PU content further would lead to continuous PU nanodomains and, as a result, decreased phase continuity of the PEGDA network. For this reason, the tensile strength increases from 2.4 to 7.5 MPa when the PU content is increased from 50 to 75% for the PU2K/PEGDA1K IPNs as well. The tensile modulus of PU2K/PEGDA# IPNs (Table I) also increases with increasing PU content. However, the tensile modulus shows maximum values (ca. 28 MPa) for the 75% PU2K/25% PEGDA1K IPN, which shows synergistic behavior.

In the case of PU1K/PEGDA# IPNs, the compositional influence on the mechanical properties of IPNs is not as significant in comparison with PU2K/PEGDA# IPNs. The tensile strength and elongation at break of PU1K/PEGDA# IPNs (Table II) gradually increase as the amount of PU is increased, whereas the tensile modulus decreases. The values for the tensile strength, tensile modulus, and elongation at break lie between 0.7 and 1.2 MPa, 3.4 and 6.8 MPa, and 16 and 40% for PU1K/PEGDA2K IPNs. Although the PU2K homonetwork has a lower crosslink density than the PU1K homonetwork, it shows much higher mechanical properties because of the existence of a crystal structure inside the PU2K homonetwork, as observed in the DSC results.

TABLE I
Tensile Properties of the Homonetworks and IPNs (M_c of PU = 2000)

Sample	Tensile strength (MPa)	Tensile modulus (MPa)	Elongation at break (%)
25% PU2K/75% PEGDA1K IPN	1.3 ± 0.2	11.0 ± 1.0	15 ± 1
50% PU2K/50% PEGDA1K IPN	2.4 ± 0.6	14.3 ± 1.2	25 ± 7
75% PU2K/25% PEGDA1K IPN	7.5 ± 1.4	27.7 ± 7.0	133 ± 32
PEGDA2K homonetwork	0.9 ± 0.1	6.2 ± 0.2	16 ± 4
25% PU2K/75% PEGDA2K IPN	1.0 ± 0.2	6.3 ± 0.3	20 ± 5
50% PU2K/50% PEGDA2K IPN	2.0 ± 0.2	9.6 ± 1.2	29 ± 7
75% PU2K/25% PEGDA2K IPN	6.5 ± 0.6	12.2 ± 0.4	158 ± 18
PU2K homonetwork	12.4 ± 0.8	11.9 ± 0.7	320 ± 10

TABLE II
Tensile Properties of the Homonetworks and IPNs (M_c of PU = 1000)

Sample	Tensile strength (MPa)	Tensile modulus (MPa)	Elongation at break (%)
25% PU1K/75% PEGDA1K IPN	0.8 ± 0.1	7.3 ± 0.3	12 ± 2
50% PU1K/50% PEGDA1K IPN	1.0 ± 0.1	3.8 ± 0.4	32 ± 5
75% PU1K/25% PEGDA1K IPN	1.6 ± 0.2	3.7 ± 0.5	62 ± 6
PEGDA2K homonetwork	0.9 ± 0.1	6.8 ± 0.7	16 ± 3
25% PU1K/75% PEGDA2K IPN	0.7 ± 0.2	4.2 ± 0.4	20 ± 5
50% PU1K/50% PEGDA2K IPN	0.8 ± 0.1	3.4 ± 0.2	26 ± 6
75% PU1K/25% PEGDA2K IPN	1.1 ± 0.2	3.5 ± 0.4	40 ± 5
PU1K homonetwork	1.2 ± 0.1	4.6 ± 0.2	35 ± 4

Swelling ratio measurement

All the IPNs in deionized water at room temperature reached equilibrium within 2 h. Generally, it has been known that the swelling behavior of a polymer blend is strongly influenced by the morphology. When IPNs show a sea-island morphology, the swelling behavior is dominated by the matrix components. If the matrix is the hydrophilic component, the IPN will show a high swelling ratio, but if the matrix is the hydrophobic component, the swelling of the hydrophilic domains inside the hydrophobic matrix is restricted, and the IPN will show restricted swelling behavior. However, if a cocontinuous morphology is obtained or if the IPN has a single intermixed phase, the swelling of the IPN will show an intermediate value between those of the hydrophilic component and hydrophobic component. The swelling ratios of PU/PEGDA IPNs fall between that of the hydrophobic PU homonetwork and that of the hydrophilic PEGDA homonetwork (not shown here), and this strongly implies cocontinuous morphology or some cocontinuity inside the IPNs. The swelling ratios of the PEGDA homonetworks and IPNs increase with the molecular weight of PEGDA increasing in the same composition because of the reduced crosslink density of PEGDA.

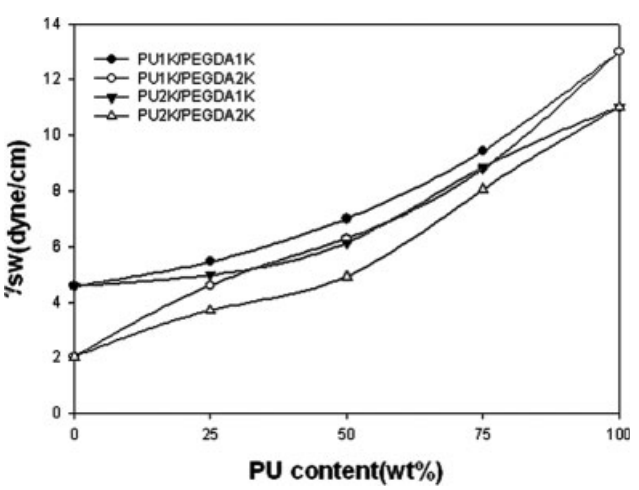

Figure 6 Contact angle with water (γ_{sw}) versus the PU content in PU/PEGDA IPNs.

Interfacial energy measurement

The interfacial energy between the samples and water was investigated with underwater contact-angle measurements. The effects of different compositions of IPNs and different crosslink densities of PEGDA and PU on the interfacial energy are shown in Figure 6. The interfacial energy of PEGDA homonetworks and PU/PEGDA IPNs increases with the molecular weight of PEGDA decreasing; that is, the hydrophilicity of the surface decreases. The results also indicate that as the content of PU, a hydrophobic component, increases, the IPN surfaces become more hydrophobic. This result of the interfacial energy measurements shows a trend similar to that of the swelling behavior in water.

AFM analysis

AFM analysis in the tapping mode was performed for all PU/PEGDA IPNs with different PU contents. The image contrast is given by the stiffness difference between the PU-rich and PEGDA-rich phases. Thus, the PEGDA-rich phase appears dark and the PU-rich phase appears bright in the images. Figures 7 and 8 show the AFM images of PU#/PEGDA1K IPNs and PU#/PEGDA2K IPNs, respectively. All IPNs show a cocontinuous morphology, which is consistent with the results for the swelling ratio in water and the surface energy measurements.

Cross-sectional images of PU#/PEGDA1K IPNs are reported in Figure 7. The aforementioned thermomechanical properties clearly indicate the phase-separated structure in these materials. Because the PEGDA network is formed first, as shown in the kinetic study,[33] the PEGDA-rich phase represents the continuous phase (matrix) in which rich PU nodules of various shapes are dispersed with some continuity in 25% PU#/75% PEGDA1K IPNs. However, with the PU content increasing up to 75%, the interconnection and domain size of the PU (bright) phase

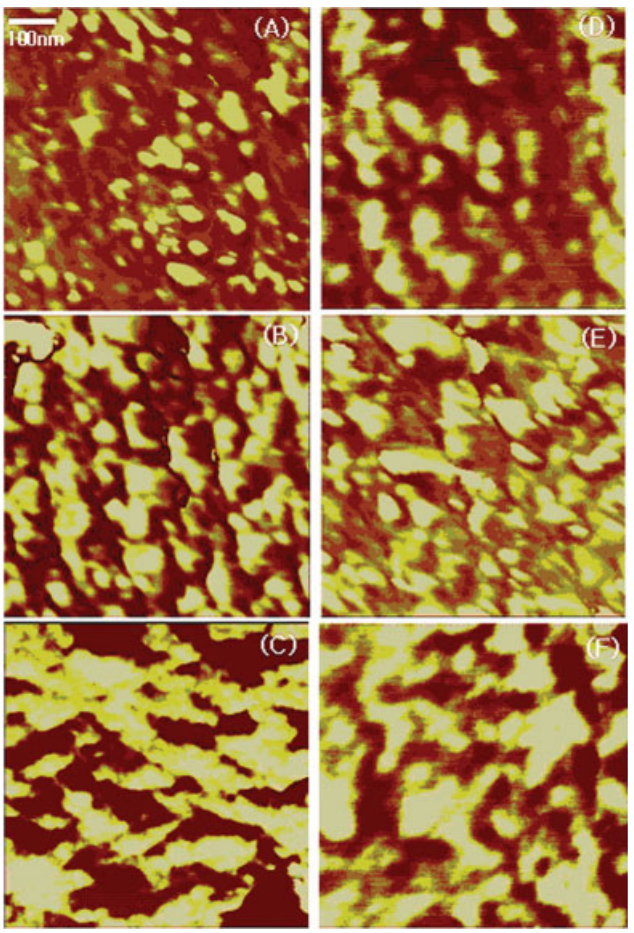

Figure 7 Cross-sectional AFM images of (A) 25% PU1K/75% PEGDA1K, (B) 50% PU1K/50% PEGDA1K, (C) 75% PU1K/25% PEGDA1K, (D) 25% PU2K/75% PEGDA1K, (E) 50% PU2K/50% PEGDA1K, and (F) 75% PU2K/25% PEGDA1K IPNs. [Color figure can be viewed in the online issue, which is available at www.interscience.wiley.com.]

are also increased. The domain size is changed from about 66 to 140 nm for PU1K/PEGDA1K IPNs.

The cross-sectional images of PU#/PEGDA2K IPNs have been also examined by AFM analysis (Fig. 8). Whether it is the predominant component or not, the PEGDA part still plays the role of the matrix. However, better interpenetration between the two phases can be observed, and the domain sizes are small, ranging from 7 to 37 nm. These results are in good agreement with the results of DMTA. Vancaeyzeele and Teyssie[34] reported that in the tan δ/temperature curve, if a single transition is located at a temperature between those of the two single networks, the domain size is considered to be of the order of 5–50 nm. The larger phase separation between the PU and PEGDA phases observed in PU#/PEGDA1K IPNs is due to the faster reaction rate of the PEGDA1K network in comparison with the PEGDA2K network. As the crosslink density of PEGDA increases (comparing PEGDA2K and PEGDA1K), the rate of PEGDA1K network formation increases, and this causes a reduction of the gel conversion and the gel time. Therefore, the time interval between PEGDA1K gelation and PU network formation also increases, and this gives more time for the PU oligomer to phase-separate and hence form larger domains. Comparing the effect of the crosslink density of PU, we see that the IPNs having the PU network with a higher crosslink density (PU1K) show smaller PU domain sizes.

CONCLUSIONS

A series of IPNs based on PU and PEGDA were prepared with the simultaneous polymerization method by the variation of the PU content from 0 to 100% and by changes in the crosslink density of PEGDA and PU from 1000 to 2000. The PU#/PEGDA1K IPNs exhibited two mechanical relaxations corresponding to the PU-rich and PEGDA-rich phases,

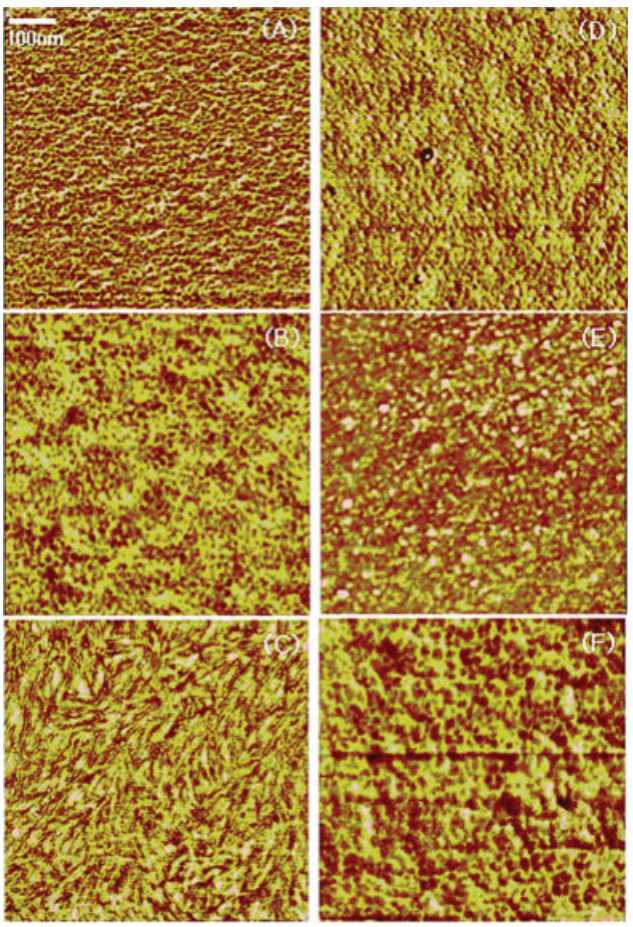

Figure 8 Cross-sectional AFM images of (A) 25% PU1K/75% PEGDA2K, (B) 50% PU1K/50% PEGDA2K, (C) 75% PU1K/25% PEGDA2K, (D) 25% PU2K/75% PEGDA2K, (E) 50% PU2K/50% PEGDA2K, and (F) 75% PU2K/25% PEGDA2K IPNs. [Color figure can be viewed in the online issue, which is available at www.interscience.wiley.com.]

which indicated the presence of two partially mixed phases caused by the faster formation of the PEGDA1K network, whereas the PU#/PEGDA2K IPNs showed single tan δ peaks, regardless of the composition, which indicated the higher degree of interpenetration between the two polymer networks. The tensile strength and elongation at break increased with increasing PU content. However, the mechanical properties of the PU2K/PEGDA# IPNs showed much higher values than those of the PU1K/PEGDA# IPNs because of the existence of a crystal structure inside PU2K, which was confirmed by the DSC analysis. Also, a particularly high increase in the tensile modulus was observed in the 75% PU2K/25% PEGDA1K IPN, which displayed synergistic behavior. The swelling ratio and contact-angle measurements of PU/PEGDA IPNs revealed that the hydrophilicity decreased with increasing PU content and with increasing crosslink density of PU and PEGDA. The swelling ratios of the IPNs fell between those of the pure PU and PEGDA homonetworks. AFM studies revealed that, as predicted from the swelling ratio results, all IPNs showed a microphase-separated cocontinuous morphology. The domain size was less than 50 nm for PU#/PEGDA2K IPNs and ranged from 66 to 140 nm for PU#/PEGDA1K IPNs. It was reported that IPNs with smaller domain sizes and higher hydrophilicity showed less platelet adhesion.[20–23] Because of the good mechanical properties and amphiphilic microphase-separated morphologies of PU2K/PEGDA2K IPNs, better blood compatibility for those materials can be expected. Also, PU2K/PEGDA2K IPNs for blood-contacting devices in a broad range of biorelated applications can be expected.

References

1. Hirose, M.; Zhou, J.; Nagai, K. Prog Org Coat 2000, 38, 27.
2. Park, Y. T.; Monterio, M. J.; Van, E. S.; German, A. L. Eur Polym J 2001, 37, 965.
3. Nakayama, Y. Prog Org Coat 1997, 31, 105.
4. Nemirovski, N.; Silverstein, M. S.; Narkis, M. Polym Adv Technol 1996, 7, 247.
5. Jean, M. R.; Henry, I.; Taha, M. J Appl Polym Sci 2000, 77, 2711.
6. Sperling, L. H. Interpenetrating Polymer Networks and Related Materials; Plenum: New York, 1981.
7. Kim, J. H.; Kim, S. C. Polym Eng Sci 1987, 27, 1252.
8. Hourston, D. J.; Schafer, F. U. J Appl Polym Sci 1996, 62, 2025.
9. Hsieh, K. H.; Liao, D. C.; Chen, C. Y.; Chiu, W. Y. Polym Adv Technol 1996, 7, 265.
10. Lee, D. S.; Kwan, S. K.; Kim, S. C. Adv Interpenetrating Polym Networks 1990, 2, 177.
11. Barrett, L. W.; Sperling, L. H. TRIP 1993, 1, 45,
12. Wang, C. B.; Cooper, S. L. Macromolecules 1981, 14, 456.
13. Sung, C. S. P.; Hu, C. B. Macromolecules 1981, 14, 212.
14. Takahara, A.; Hergenrother, R. W.; Coury, A. J.; Cooper, S. L. Artif Organs 1990, 14, 87.
15. Lyman, D. J.; Metcalf, L. C.; Albo, D., Jr.; Richard, K. F.; Lamb, J. Trans Am Soc Artif Int Organs 1974, 20, 474.
16. Tyler, B. J.; Ratner, B. D. J Biomed Mater Res 1993, 27, 327.
17. Shin, Y. C.; Han, D. K.; Kim, Y. H.; Kim, S. C. J Biomater Sci Polym Ed 1994, 6, 195.
18. Shin, Y. C.; Han, D. K.; Kim, Y. H.; Kim, S. C. J Biomater Sci Polym Ed 1994, 6, 281.
19. Roh, H. W.; Song, M. J.; Han, D. K.; Ahn, D. S.; Lee, J. H.; Kim, S. C. J Biomater Sci Polym Ed 1999, 10, 123.
20. Kim, J. H.; Song, M. J.; Roh, H. W.; Shin, Y. C.; Kim, S. C. J Biomater Sci Polym Ed 2000, 11, 197.
21. Kim, J. H.; Kim, S. C. Biomaterials 2002, 23, 2015.
22. Kim, J. H.; Kim, S. C. Macromolecules 2003, 36, 2867.
23. Yoon, S. S.; Kim, J. H.; Kim, S. C. Polym Bull 2005, 53, 339.
24. Amiji, M.; Park, K. J Biomater Sci Polym Ed 2003, 14, 601.
25. Jo, S. B.; Shin, H. S.; Shung, A. K.; Fisher, J. P.; Mikos, A. G. Macromolecules 2001, 34, 2839.
26. Hepbure, C. Polyurethane Elastomers, 2nd ed.; Elsevier: New York, 1995.
27. Padmavathi, N. C.; Chatterji, P. R. Macromolecules 1996, 29, 1976.
28. Andrade, J. D.; Ma, S. M.; King, R. N.; Gregois, D. E. J Colloid Interface Sci 1979, 72, 488.
29. Van Krevelen, D. W. Properties of Polymers, 3rd ed.; Elsevier: New York, 1990.
30. Schrader, M. E.; Loeb, G. I. Modern Approaches to Wettability; Plenum: New York, 1992.
31. Hourston, D. J.; Schafer, F. U. Polymer 1996, 37, 3521.
32. Perera, M. C. S. Polymer 1999, 40, 1667.
33. Klempner, D.; Berkowsky, L. Encyclopedia of Polymer Science and Engineering; Wiley: New York, 1998; p 8.
34. Vancaeyzeele, C.; Teyssie, D. Polymer 2006, 47, 6048.